

ORIGINAL ARTICLE

Ingested D-Aspartate Facilitates the Functional Connectivity and Modifies Dendritic Spine Morphology in Rat Hippocampus

Akihiko Kitamura^{1,†}, Yasushi Hojo^{2,†}, Muneki Ikeda³, Sachise Karakawa¹, Tomomi Kuwahara¹, Jonghyuk Kim³, Mika Soma³, Suguru Kawato³ and Tomokazu Tsurugizawa⁴

¹Institute for Innovation, Ajinomoto Co., Inc., Suzuki-cho 1-1, Kawasaki-ku, Kawasaki 2108681, Japan,

²Department of Biochemistry, Faculty of Medicine, Saitama Medical University, Saitama 3500495, Japan,

³Department of Cognitive Neuroscience, Faculty of Pharma-Science, Teikyo University, Kaga 2-11-1, Itabashi, Tokyo 1738605, Japan and ⁴NeuroSpin, CEA-Saclay Center, Gif-sur-Yvette 91191, France

Address correspondence to Tomokazu Tsurugizawa, NeuroSpin, Commissariat à l'Energie Atomique et aux Energies Alternatives, CEA Saclay, Gif-sur-Yvette, France. Email: tsurugizawa@gmail.com. Suguru Kawato, Department of Cognitive Neuroscience, Faculty of Pharma-Science, Teikyo Univ., Kaga 2-11-1, Itabashi, Tokyo 1738605, Japan. Email: kawato@bio.c.u-tokyo.ac.jp

[†]These authors contributed equally to this work.

Abstract

D-Aspartate (D-Asp), the stereoisomer of L-aspartate, has a role in memory function in rodents. However, the mechanism of the effect of D-Asp has not been fully understood. In this study, we hypothesized that ingested D-Asp directly reaches the hippocampal tissues via the blood circulation and modifies the functional connectivity between hippocampus and other regions through spinogenesis in hippocampal CA1 neurons. The spinogenesis induced by the application of D-Asp was investigated using rat acute hippocampal slices. The density of CA1 spines was increased following 21 and 100 μ M D-Asp application. The nongenomic spine increase pathway involved LIM kinase. In parallel to the acute slice study, brain activation was investigated in awake rats using functional MRI following the intragastric administration of 5 mM D-Asp. Furthermore, the concentration of D-Asp in the blood serum and hippocampus was significantly increased 15 min after intragastric administration of D-Asp. A functional connectivity by awake rat fMRI demonstrated increased slow-frequency synchronization in the hippocampus and other regions, including the somatosensory cortex, striatum, and the nucleus accumbens, 10–20 min after the start of D-Asp administration. These results suggest that ingested D-Asp reaches the brain through the blood circulation and modulates hippocampal neural networks through the modulation of spines.

Key words: D-aspartate, functional MRI, hippocampus, rats, spine morphology

Introduction

D-aspartate (D-Asp), which is the stereoisomer of L-aspartate (L-Asp), has received significant attention for its function as a neurotransmitter in the mammalian nervous system (Schell

et al. 1997; Furuchi and Homma 2005; D'Aniello 2007; Homma 2007). D-Asp has been shown to be present in the rat brain as well as in neuroendocrine tissues, such as the adrenal medulla and the testes (Dunlop et al. 1986; Hashimoto et al. 1993).

In adults, D-Asp exists in the neurons in the dentate gyrus, where new neurons are generated (Ming and Song 2005). Recently, the existence of D-Asp in natural products, such as *Anadara broughtonii*, has been reported (Sato et al. 1987), and the oral intake of D-Asp (40 mM) for 12–16 days improves rats' cognitive ability to find a hidden platform in the Morris water maze test (Topo et al. 2010). D-Asp also rescues age-related deterioration of hippocampal synaptic plasticity in mice, implying an intriguing possibility that it can counteract the age-related reduction of NMDA receptor signaling (Errico et al. 2011). These results imply that the oral intake of D-Asp would exert an effect on memory function through interaction with hippocampal neurons. On the other hand, our previous study indicated that intragastric administration of L-Asp did not activate hippocampus (Tsurugizawa et al. 2014). Additionally, there has been no study to investigate the effect of acute D-Asp intake on brain function.

On the microscale, the regulation of spinogenesis in hippocampal neurons is an important factor in memory processes in that it increases the number of spines for the sake of new synaptic contacts (Hering and Sheng 2001). Rapid spinogenesis occurs in 2 h in response to increased neuronal activity or neurosteroids (Maletic-Savatic et al. 1999; Mukai et al. 2007; Hasegawa et al. 2015; Hojo et al. 2015). However, there has been no report on the effect of D-Asp on spinogenesis in hippocampal neurons. On the macroscale, functional MRI (fMRI) is a promising tool to investigate neuronal activity in the rat brain comprehensively. Particularly, resting state fMRI focuses on low-frequency synchronization (0.01–0.1 Hz) among the brain regions, known as functional connectivity (Lee et al. 2013). Previously, we successfully showed regional activation depending on intragastrically administered chemical substances in “awake” rat fMRI (Tsurugizawa et al. 2009, 2010a, 2013; Tsurugizawa and Uneyama 2014; Uematsu et al. 2015). The merit of awake fMRI is that it removes the effect of anesthetics not only on neurovascular coupling (Tsurugizawa et al. 2010b) but also on consciousness (Abe et al. 2017).

In the current study, we aimed to investigate 1) D/L-amino acid level changes in the serum and in the hippocampus and 2) low-frequency synchronization between the hippocampus and other regions following the intragastric administration of D-Asp using awake fMRI in rats. Furthermore, we investigated 3) spinogenesis in pyramidal neurons in acute hippocampal slices in response to D-Asp application.

Materials and Methods

Animals

Measurements of BOLD were performed using 17 male Wistar rats (10 weeks old at the start of surgery, Charles River Laboratories, Yokohama, Japan) for D-Asp ($n = 11$) or physiological saline ($n = 6$) infusion. The plasma and brain tissue amino acid levels were determined using 18 male Wistar rats (11–12 weeks old, Charles River Laboratories) with no intragastric administration (control condition, $n = 9$) or 15 min after D-Asp infusion ($n = 9$). The rats were housed individually in wire-mesh cages under controlled temperature ($23 \pm 0.5^\circ\text{C}$) and light (7:00–19:00) conditions with free access to water and food (CRF-1, Oriental Yeast, Tokyo, Japan). All in vivo animal procedures in the present study were approved by the Committee for Animal Experiments at Ajinomoto Co., Inc., and were carried out in accordance with the guidelines of the US NIH regarding the care and use of animals for experimental procedures.

Surgery

To perform awake fMRI measurements, we subjected rats to cranioplastic surgery (Tsurugizawa et al. 2010b) under 1.5% isoflurane (Abbott, Abbott Park, IL, USA). Briefly, for intragastric cannulation, one end of a silicon tube was passed from the abdomen under the back skin and secured on the head. To attach a head post without anchors, we applied a resin cement (Super-Bond C&B, Sun Medical Company, Ltd., Moriyama, Japan) to the surface of the skull. Then, cranioplastic resin cement (Unifast TRAD, GC Corporation, Tokyo, Japan) was applied to the skull, and a plastic pole (7 mm diameter, 30 mm length), which could be used for head fixation without pain during the imaging session, was vertically fixed with acrylic cement. The other end of the silicone tube was inserted into the gastric fundus and ligated with a silk thread. Following surgery, the rats were allowed to recover for more than 1 week.

Acclimation Training

We used the acclimation method as described previously (Tsurugizawa et al. 2010b). To allow the rats to adapt to the awake MRI condition, they were trained for 5 days at the same time each day (10:00–17:00) to minimize effects due to circadian rhythm. During the first 3 days, a pseudo-MRI system was used, which consisted of a nonmagnet bore and head positioner. At first, the rats were lightly anesthetized for a short time using 1.5% isoflurane. The rats were then immediately set into the head positioner and fixed in place by the cranioplastic acrylic head mount with the plastic pole. Their bodies were gently restrained with elastic bands and their limbs were allowed to move freely. To reduce stress due to noise, earplugs were used throughout the experiment. The rats were then left in the pseudo-fMRI apparatus for 30 min on the first day and for 90 min on the second and third days after recovery from anesthesia. These conditions and an actual MRI machine were used for the next 2 days. Throughout training, the heart and respiration rates were measured using an MR-compatible monitoring system (Model 1025, SA Instruments, NY, USA). We confirmed that the measurement of physiological parameters reflecting the stress level in rats, such as the respiration rate and the heart rate were not significantly different from normal levels at the last day of acclimation training ($P > 0.05$ by *t*-test), in consistent with our previous study (Tsurugizawa et al. 2010b). Additionally, the shape feces was normal (no diarrhea and normal softness). These showed that acclimation training minimizes the stress induced via MRI scanning.

Awake fMRI

All MRI measurements were performed after the rats were fasted for 12–15 h, and body temperature was maintained between 36°C and 37°C by circulating water throughout the experiment. The rats were anesthetized for a short time with 1.5% isoflurane. The cranioplastic acrylic mounting was then immediately fixed with a plastic bar (avoiding the painful insertion of ear bars) on a nonmagnetic stereotaxic apparatus. Scanning was then initiated. The studies utilized a Bruker AVANCE III system (Bruker, Ettlingen, Germany) with a 4.7 T/40 cm horizontal superconducting magnet equipped with gradient coils (12 cm diameter). The BOLD fMRI data were obtained using a T2*-weighted multislice echo-planar imaging (EPI) sequence with the following parameters: time of repetition = 4 s, echo time = 10 ms, field of view = $32\text{ mm} \times 32\text{ mm}$, acquisition matrix = 80×80 , slice thickness = 1.0 mm, and slice

number = 20. Structural images were obtained via a multislice rapid acquisition with relaxation enhancement (RARE) sequence using the following parameters: time of repetition = 2500 ms, effective echo time = 60 ms, RARE factor = 8, acquisition matrix = 128 × 128 and 4 averages. Ten minutes after the scanning began, a 5 mM D-Asp (Wako, Osaka, Japan) or 0.9% NaCl (Wako, Osaka, Japan) solution was delivered into the stomach via an implanted tube for 1 min for 10 mL/kg body weight by means of a syringe pump (CVF-3200, Nihon Kohden, Tokyo, Japan) (Fig. 1).

Data Preprocessing

SPM8 software (Wellcome Trust Centre for Neuroimaging, UK) was used for preprocessing, including realignment, coregistration to structural images, and spatial normalization of functional data. Before preprocessing, template images coregistered to the Paxinos and Watson rat brain atlas were obtained (Paxinos and Watson 1998).

BOLD Signal Change

The brain regions demonstrating significant BOLD changes were identified by applying boxcar functions in SPM8. The “off” period of the boxcar function was the basal period, corresponding to the 5-min period before the start of nutrient administration, and the “on” period was the period of potential activation, which corresponded to the 5-min period after the start of administration (Fig. 1). The activation map was thresholded at $P < 0.05$ (FWE corrected).

Functional Connectivity

The resting state fMRI data analysis toolkit (REST1.8, Lab of Cognitive Neuroscience and Learning, Beijing Normal University, China) and SPM8 software were used to analyze the fMRI data. We used cross-correlation analysis between averaged time courses of BOLD signals within regions of interest (ROIs), which were drawn manually based on the structural images with reference to the mouse brain atlas. The functional connectivity before (0–5 min before D-Asp administration) and after administration

of D-Asp (15–20 min after the start of application) within each ROI was calculated from the fMRI data. As we were only interested in the temporal correlation due to slow periodic spontaneous oscillations, a bandpass filter (0.01–0.1 Hz) was used to exclude the high-frequency components from each of the data sets following the preprocessing described above. Head motion traces and mean signals in the ventricles and white matter were regressed out of each of the time-series to reduce contributions from physiological noise. We confirmed that the motion levels were less than one-third of pixel throughout the scanning in all rats. In a pixel-by-pixel analysis based on the hippocampus, the correlation coefficient map with an averaged time course in the hippocampus was calculated for each individual rat. Then, group statistical mapping of the correlation coefficient was performed in SPM8. In ROI-ROI analysis, the averaged time courses in several ROIs—the somatosensory cortex, hippocampus, caudate putamen, substantia nigra, and nucleus accumbens—were extracted and the correlation coefficient calculated in each individual rat. The ROIs were selected based on the previous articles that showed the connection between hippocampus (Pennartz et al. 2011; Xie et al. 2013). Then, the differences between before and after D-Asp administration were assessed for statistical significance by means of paired t-tests.

Blood Sample Collection and Brain Tissue Collection

In studies separate from the MRI experiments, plasma and brain tissue amino acids levels were measured. The rats were gavaged with 5 mM D-Asp at a volume of 1 mL/100 g body weight. Then, the rats were deeply anaesthetized with isoflurane and decapitated. Immediately after decapitation, the blood sample was collected. The brain was removed from the skull, and the hippocampus was isolated from the brain.

Quantification of D/L-Amino Acid Concentrations in the Plasma and Brain Tissue

The blood sample was collected in a heparinized tube and centrifuged at 3000 rpm for 15 min at 4 °C to obtain the plasma. The plasma sample (20 μL) was mixed with 20 μL of the internal standard solution (stable isotope-labeled D/L-amino acids in water) and 40 μL of MeCN. The mixture was centrifuged at 12 000 rpm for 10 min at 20 °C, and the supernatants were collected. Hippocampal brain tissue was collected and quickly frozen in liquid nitrogen, then stored at –80 °C. The frozen tissue was powdered using a Multi-Beads Shocker (Yasui Kikai, Osaka, Japan) and homogenized in an ice-cold 80% MeOH aqueous solution containing stable isotope-labeled D- and L-amino acids as the internal standard (to correct the extraction of amino acids from tissues) at a concentration of 10 mg wet tissue/mL. The homogenate (400 μL) was further mixed with 400 μL of water and 400 μL of chloroform, then centrifuged at 12 000 rpm for 5 min at 4 °C. A portion of the supernatant (600 μL) was transferred to a sample tube and dried under reduced pressure, then redissolved in 60 μL of water. A previously described quantification method for D/L-amino acids (Visser et al. 2011) was used in this study with minor modifications. The amino acids in the samples were derivatized with (S)-NIFE as follows. The sample solution (20 μL) from the tissue was dissolved in 20 μL of 200 mM sodium borate buffer (pH 8.8), then 20 μL of 5 mg/mL (S)-NIFE in MeCN was added and incubated for 10 min at room temperature. An aqueous 0.1 M solution of hydrochloric acid (40 μL) was then added, and 3 μL of the reaction mixture was subjected to LC-MS-MS. The derivatized amino acids were

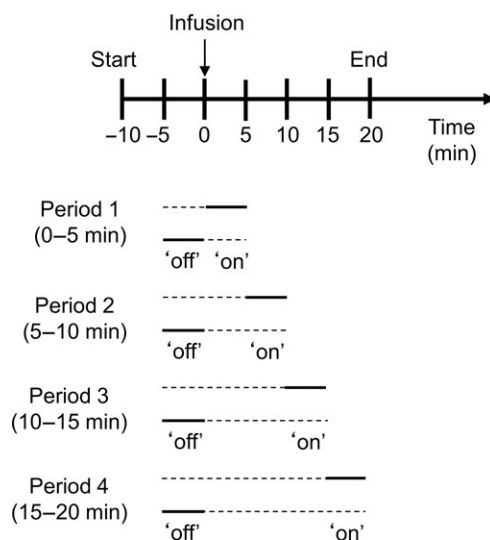


Figure 1. Schematic figure of the experimental protocol for awake fMRI. fMRI scanning was started 10 min before D-Asp administration. D-Asp was administered intragastrically at 0 min, and then scanning continued for 20 min.

separated on an Acquity UPLC BEH C18 column (2.1 × 100 mm, Waters, Milford, MA, USA). The mobile phase was a mixed solution of eluent A (10 mM ammonium hydrogen carbonate in water (pH 9.5)) and eluent B (acetonitrile). The Nexera X2 HPLC system from Shimadzu (Kyoto, Japan) and the Sciex Triple Quad 6500 MS/MS system (Sciex, Framingham, MA, USA) were used. Sciex Analyst 1.6.2 software was used to control these instruments and to quantitate each amino acid. The Smirnov–Grubbs test was used to detect outliers. Any data that were statistically rejected by the Smirnov–Grubbs test were excluded as outlier data.

Imaging and Analysis of Dendritic Spine Density and Morphology

Hippocampal Slice Preparation and Current Injection of Lucifer Yellow

Male rats aged 12 weeks were deeply anesthetized and decapitated. The brains were removed and placed in artificial cerebrospinal fluid (ACSF) at 4 °C. ACSF consisted of (mM) 124 NaCl, 5.0 KCl, 1.25 NaH₂PO₄, 2.0 MgSO₄, 2.0 CaCl₂, 22 NaHCO₃, and 10 glucose and was equilibrated with 95% O₂/5% CO₂. The hippocampus was dissected, and 400 μm thick slices transverse to the long axis were cut from the middle third of the hippocampus with a vibratome (Dosaka, Japan). These “fresh” hippocampal slices were transferred into an incubating chamber containing ACSF held at 25 °C for 2 h for slice recovery. The resultant “acute” slices (used worldwide) were then incubated with D-Asp (Wako, Osaka, Japan) or together with an inhibitor of LIM kinase (10 μM) for 2 h (LIMKi, Wako, Osaka, Japan). The slices were incubated for 2 h, because we had observed a significant increase in spine density after 2 h of 17β-estradiol in a previous study (Hasegawa et al. 2015). Slices were then fixed with 4% paraformaldehyde in PBS at 4 °C overnight. Neurons within slices were visualized by an injection of Lucifer yellow (Molecular Probes, USA) under a Nikon E600FN microscope (Japan) equipped with a C2400-79H infrared camera (Hamamatsu Photonics, Japan) and a ×40 water immersion lens (Nikon, Japan). Current injection was performed with a glass electrode filled with 5% Lucifer yellow for 10 min using Axopatch 200B (Axon Instruments, USA). Approximately 2–3 neurons within a depth range of 20–30 μm from the surface of a slice were injected with Lucifer yellow.

Confocal Laser Microscopy and Morphological Analysis

The imaging was performed from sequential z-series scans with a confocal laser scanning microscope (LSM5; Carl Zeiss, Germany) at high zoom (×3.0) with a ×63 water immersion lens, NA 1.2. For Lucifer yellow, the excitation and emission wavelengths were 488 and 530 nm, respectively. For analysis of the spines, a 3D image was reconstructed from approximately 40 sequential z-series sections taken every 0.45 μm with a ×63 water immersion lens, NA 1.2. The applied zoom factor (×3.0) yielded 23 pixels per 1 μm. The confocal lateral resolution was approximately 0.16 μm. The z-axis resolution was approximately 0.47 μm. Our resolution limits were regarded as sufficient to allow the determination of spine density. Confocal images were then deconvoluted using AutoDeblur software (AutoQuant, USA).

The density of spines as well as the head diameter were analyzed with Spiso-3D (an automated software mathematically calculating geometrical parameters of spines), developed by the Bioinformatics Project of Kawato’s group (Mukai et al. 2011). Spiso-3D has equivalent capacity to NeuroLucida (MicroBrightField, USA); furthermore, Spiso-3D considerably reduces human error and

experimenter labor. The single apical dendrite was analyzed separately. The spine density was calculated from the number of spines along secondary dendrites with a total length of 40–60 μm. These dendrites were present within the stratum radiatum, between 100 and 200 μm from the soma. Spine shapes were classified into 3 categories as follows: 1) small-head spines, with a head diameter between 0.2 and 0.4 μm; 2) middle-head spines, which have 0.4–0.5 μm spine heads; and 3) large-head spines, with a head diameter between 0.5 and 1.2 μm. Small-, middle-, and large-head spines may differ in their number of AMPA receptors, and therefore these 3 types of spines may have different degrees of efficiency in signal transduction. The number of AMPA receptors (including the GluR1 subunit) in the spine increases as the size of the postsynaptic surface increases, whereas the number of NMDA receptors (including the NR2B subunit) may be relatively constant (Shinohara et al. 2008). Because the majority of spines (>93–95%) had a distinct head, and stubby spines and filopodia did not contribute much to overall changes, we analyzed spines having a distinct head.

Results

Intragastric Administration of D-Asp Increased Hippocampal Activity

Figure 2 depicts the temporal and spatial pattern of significant BOLD changes during the intragastric administration of D-Asp or saline in awake rats. The intragastric infusion of D-Asp significantly increased the BOLD signals in several regions, including the hippocampus, hypothalamus, caudate putamen, thalamic nuclei, and motor cortex, mostly after 10 min from the start of administration (Fig. 2A). This BOLD signal increase continued through the end of scanning (20 min from the start of the D-Asp administration). Physiological saline did not increase BOLD signals significantly (Fig. 2B). The number of voxels that had a significant BOLD increase ($P < 0.05$, FWE corrected) after D-Asp administration was calculated from the result of Figure 2A (Fig. 2C). The number of significant positive BOLD signal changes ($P < 0.05$, FEW corrected) was increased in periods 3 and 4 compared with periods 1 and 2.

Intragastric Administration of D-Asp Augmented the Resting-State Functional Connectivity on the Hippocampus

Next, we assessed the resting state functional connectivity in several regions, including the hippocampus, before and after D-Asp infusion. Figure 3A provides horizontal maps of the functional connectivity based on the seed of hippocampus (red area). Before administration, significant correlation with the averaged signal fluctuation in the whole hippocampus was scattered in the cortex (blue area) and the hippocampus (red area). In contrast, after D-Asp administration, the correlated regions to the hippocampus were observed in the wide range of hippocampus and were extended to the cortex. The ROI-based functional connectivity highlighted the significant increase in the correlation coefficient of low-frequency fluctuation between the hippocampus and several other regions bilaterally, namely, the somatosensory cortex, nucleus accumbens, substantia nigra, and caudate putamen (Fig. 3B,C). In addition to the hippocampus, the correlation coefficient with the nucleus accumbens was increased in the somatosensory cortex and caudate putamen bilaterally. We confirmed that head-displacement, respiration

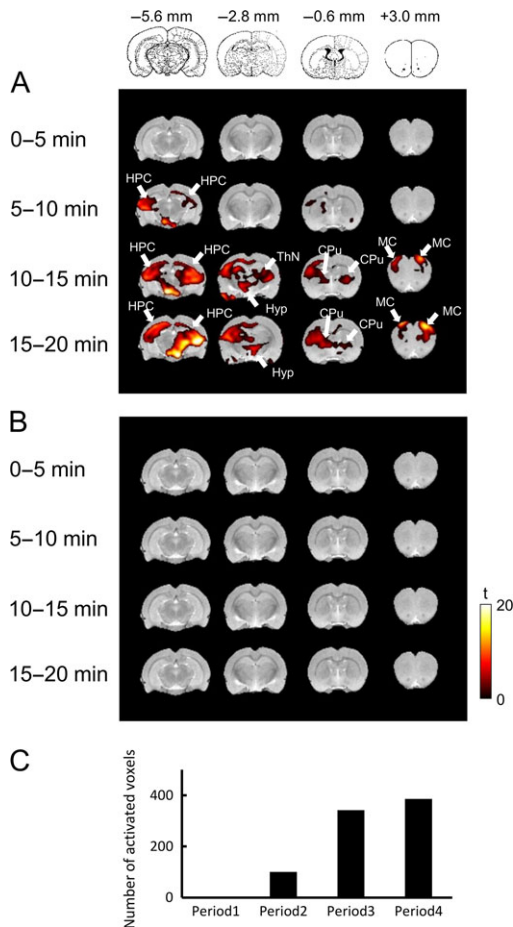


Figure 2. (A, B) Areas of the awake rat brain that had significant BOLD signal changes in response to D-aspartate administration (A) and physiological saline (B) ($P < 0.05$, FEW-corrected). t-map images depict the areas with significant increases in BOLD signal intensity. t-Values show the significant changes in BOLD signal intensity compared with the preadministration period (5 min before the infusion). (C) The number of pixels with significant BOLD increase by D-Asp administration, which was calculated from the result of Figure 2A. Color bar represents t-value. Cpu, caudate putamen; HPC, hippocampus; MC, motor cortex; ThN, thalamic nuclei; Hyp, hypothalamus.

rate, and heart rate did not significantly change between before and after D-Asp administration ($P > 0.05$ by paired t-test).

Intragastric Administration of D-Asp Increased D-Asp Concentration in the Blood Serum and the Hippocampus

Blood Serum

The changes in blood serum amino acid levels are shown in Figure 4. The D-Asp concentration was significantly increased 15 min after intragastric administration of D-Asp ($3.28 \pm 0.58 \mu\text{M}$) compared with the control ($0.35 \pm 0.03 \mu\text{M}$, $P = 0.0009$). There were no significant differences in D-Ala, D-Ser, L-Ala, L-Asp, or Gly between the control and 15 min after administration.

Hippocampus

The changes in hippocampal amino acid levels are shown in Figure 5. The D-Asp concentration was significantly increased 15 min after intragastric administration of D-Asp ($21.29 \pm 1.23 \text{ nmol/g wet tissue}$) compared with the control ($18.28 \pm 0.600 \text{ nmol/g wet tissue}$, $P = 0.049$). There were no significant

differences in D-Ala, D-Ser, L-Ala, L-Asp, L-Ser, or Gly between the control and 15 min after administration.

Rapid Effect of D-Asp on CA1 Spinogenesis via LIM Kinase

We investigated the rapid nongenomic effect of D-Asp on the modulation of dendritic spine density and morphology. Two hours after treatments with $21 \mu\text{M}$ and $100 \mu\text{M}$ D-Asp (Fig. 6A), the total spine density was significantly increased from 1.04 ± 0.04 spines/ μm (control group) to 1.16 spines/ μm ($21 \mu\text{M}$ D-Asp, $P = 0.0314$ vs. control) and 1.35 ± 0.04 spines/ μm ($100 \mu\text{M}$ D-Asp, $P = 0.0018$ vs. control) (Fig. 6B). As LIM kinase (LIMK) signaling is essential for the regulation of spine morphology via the polymerization/depolymerization of actin (Hasegawa et al. 2015; Ikeda et al. 2015), we addressed whether LIMK signaling contributes to D-Asp-induced spinogenesis. The application of an inhibitor of LIMK (LIMKi) suppressed the $100 \mu\text{M}$ D-Asp-induced increase in the total density of spines (0.95 ± 0.08 spines/ μm) ($P = 0.0008$, $100 \mu\text{M}$ D-Asp vs. D-Asp + LIMKi) (Fig. 6B). For morphological analysis, the spines were classified into 3 categories, including small-, middle-, and large-head spines. The population of middle-head spines was significantly increased following 2 h of $100 \mu\text{M}$ D-Asp treatments (0.52 ± 0.04 spines/ μm in control and 0.77 ± 0.03 spines/ μm in $100 \mu\text{M}$ D-Asp, $P = 0.0004$ vs. control) (Fig. 6C,D). The application of LIMKi significantly suppressed $100 \mu\text{M}$ D-Asp induced increase in middle-head spines (0.41 ± 0.04 spines/ μm) ($P < 0.0001$, $100 \mu\text{M}$ D-Asp vs. D-Asp + LIMKi) (Fig. 6C,D). There was no significant change in the number of small-head or large-head spines with the application of $100 \mu\text{M}$ D-Asp or $100 \mu\text{M}$ D-Asp + LIMKi.

Discussion

Findings in This Study

In the current study, we showed that 1) intragastrically administered D-Asp reached the hippocampus in 15 min via blood circulation and that 2) D-Asp augmented the slow-frequency synchronization between the hippocampus and other regions, including the somatosensory cortex, caudate putamen, nucleus accumbens, and substantia nigra, in rats. Furthermore, 3) D-Asp treatment induced the spinogenesis of middle size of spines, which are important for synaptic connections, within 2 h in rat hippocampal CA1 neurons. These results indicate that ingested D-Asp directly interacts with the hippocampus, facilitating the functional network associated with memory function.

Combination of Awake fMRI and Spine Morphology: Macroscale and Microscale

It has been shown that anesthesia depresses the conscious state in rodents, although it is widely used to suppress the motion artifact in rodent fMRI. For this reason, there exists a significant gap between rodent fMRI and human fMRI because human fMRI does not use anesthesia and therefore can investigate higher-order of the brain function, such as memory and cognition. In research including our previous study, awake rat fMRI has been developed as a method to detect the brain regions related to behavior and memory tasks without the interference of anesthesia (Tsurugizawa et al. 2010b; Pan et al. 2015; Chang et al. 2016; Yoshida et al. 2016). For instance, the regions associated with reward are activated during the presentation of a conditioned stimulus (Tsurugizawa et al. 2012). The functional connectivity among the amygdala, prelimbic cortex,

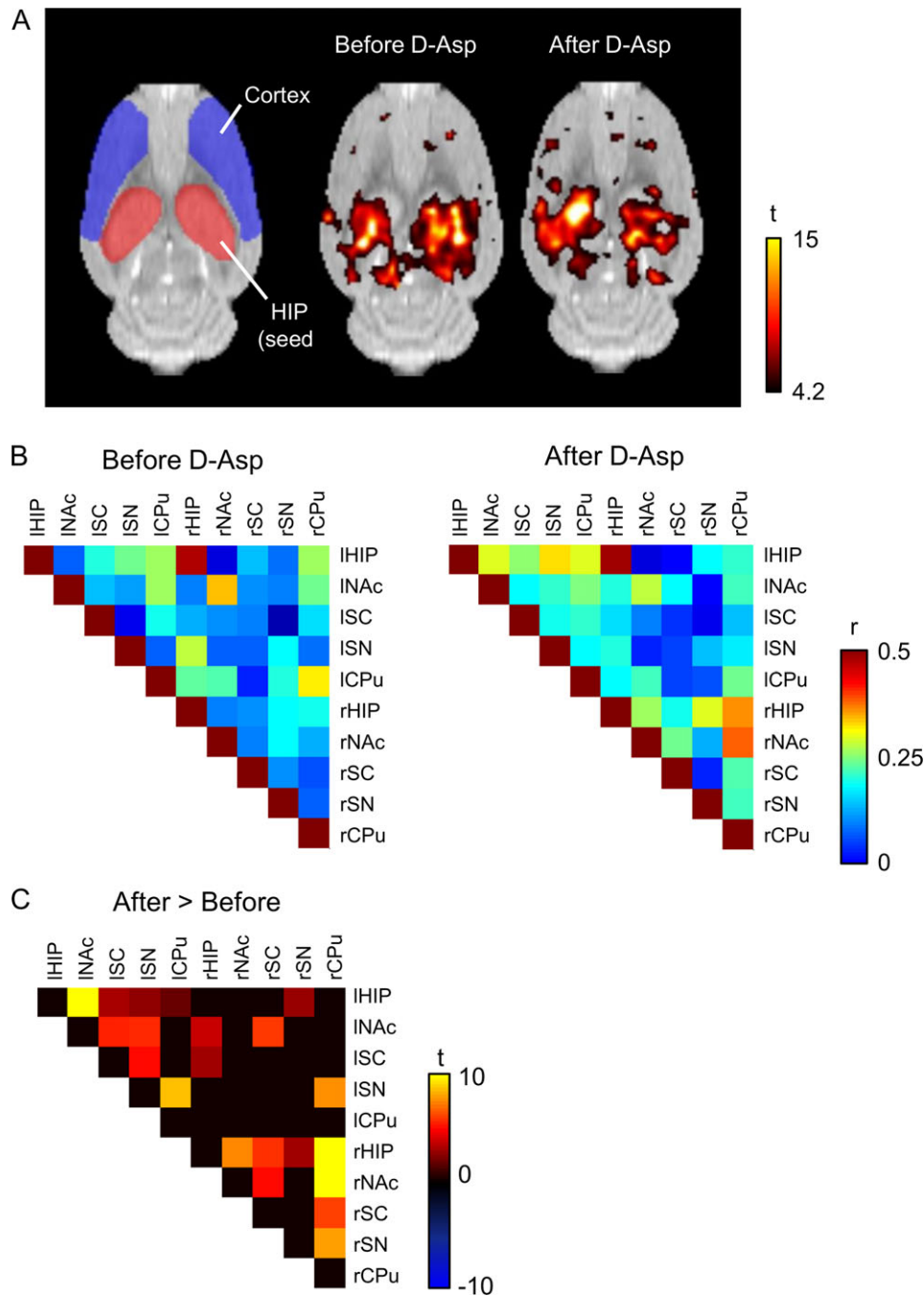


Figure 3. (A) Functional connectivity based on the hippocampus (seed, red). Blue regions represent the cortex ($P < 0.05$, FWE corrected). (B) ROI-ROI correlation coefficient matrices before and after administration of D-Asp. Color bar represents the correlation coefficient. (C) ROI-ROI t-value matrices between the correlation coefficients before and after D-Asp administration. Color bar represents t-value ($P < 0.05$, Bonferroni corrected). l/rHIP, left/right hippocampus; l/rNAC, left/right nucleus accumbens; l/rSC, left/right somatosensory cortex; l/rCPu, left/right caudate putamen; l/rSN, left/right substantia nigra.

and insular cortex changes during conditioned taste aversion (Uematsu et al. 2015). Present awake fMRI would possibly thus reflect the brain activity associated with memory function.

In the present study, we successfully examined the effect of D-Asp on macroscale low-frequency synchronization in awake rat fMRI and on microscale postsynaptic morphology, which is important in the neuronal plasticity involved in memory (Segal 2005), in acute hippocampal slices. The increased synchronization between the hippocampus and other regions is inferred to result from spinogenesis in CA1 neurons. This multiscale study

advances the field of rodent fMRI to provide more forward translational approach regarding the mechanism of brain function. Here, we observed rapid nongenomic spinogenesis after 2 h of incubation with D-Asp. Previously, we observed spinogenesis after 2 h of incubation with 17β -estradiol and testosterone through the LIMK pathway (Mukai et al. 2007; Hatanaka et al. 2015), supporting our result. Nevertheless, the current study did not investigate acute D-Asp effect on the memory function in adult or aged rats. Further experiments are required to clarify the acute D-Asp effects.

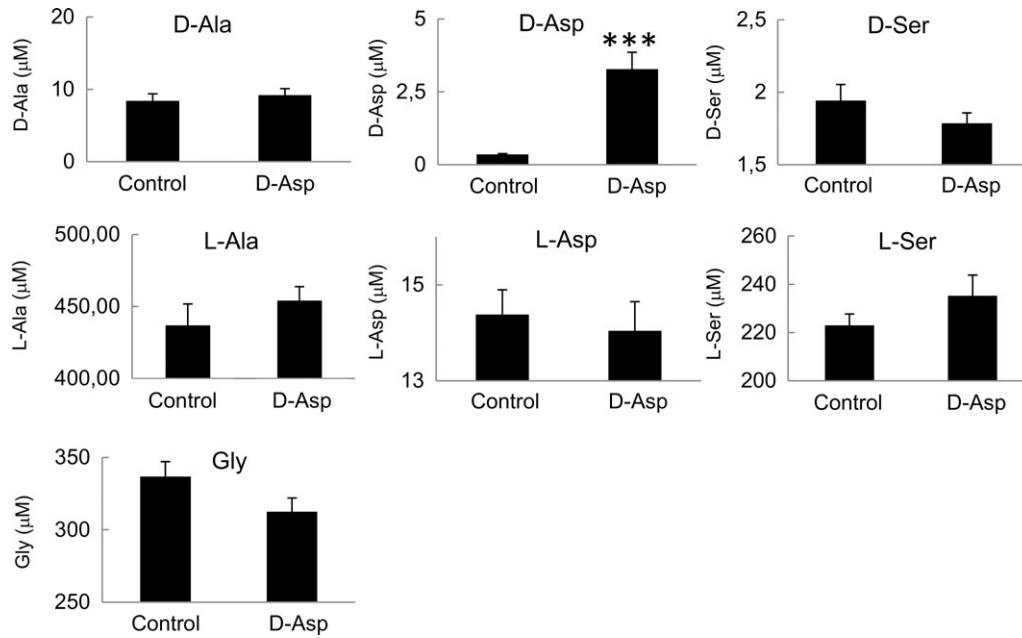


Figure 4. The changes in D/L-alanine (D/L-Ala), D/L-aspartate (D/L-Asp), D/L-serine (D/L-Ser), and glycine levels in the serum 15 min after the intragastric administration of D-aspartate. Data are expressed as the mean \pm SEM. *** $P < 0.001$ by t-test.

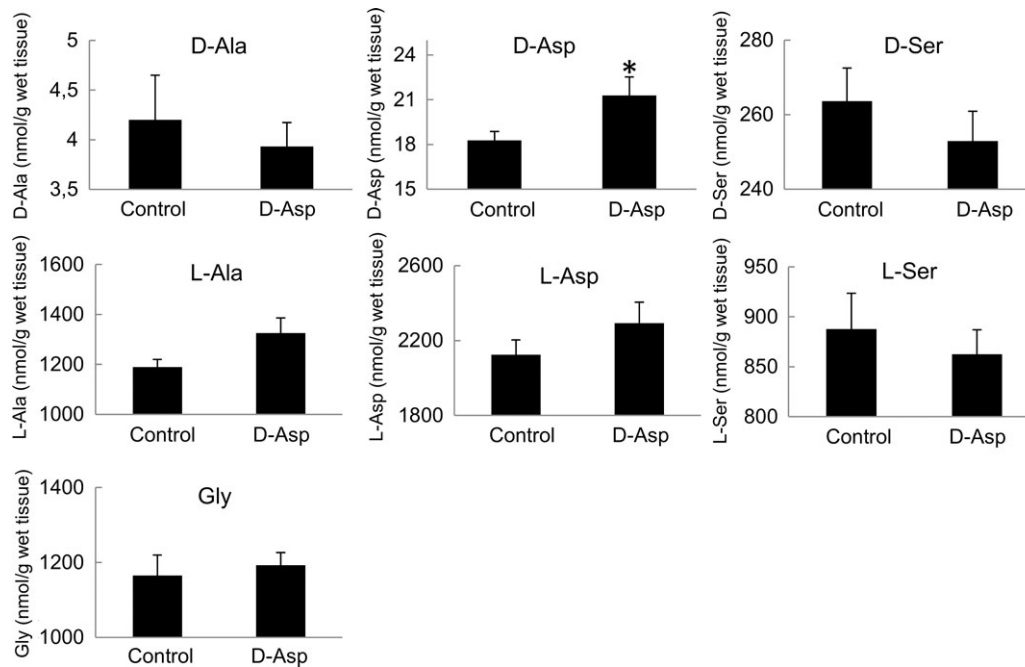


Figure 5. The changes in D/L-alanine (D/L-Ala), D/L-aspartate (D/L-Asp), D/L-serine (D/L-Ser), and glycine levels in the hippocampus 15 min after the intragastric administration of D-aspartate. Data are expressed as the mean \pm SEM. * $P < 0.05$ by t-test.

D-Asp Concentration in the Brain

In the current study, intragastric administration of D-Asp increased both plasma and hippocampal D-Asp. In the previous study, the intravenously injected D-Asp was also delivered to the hippocampus (Morikawa et al. 2007), and the D-Asp transporter has been identified previously (Kanai and Hediger 2003). These reports support our results.

Are the concentrations used for intragastric administration in vivo and bath application ex vivo sufficiently close to the

physiological range? D-Asp exists in many types of bivalves, such as *Scapharca broughtonii* and *Crassostrea nippona* (Shibata et al. 2001). The concentration of D-Asp in the bivalve is approximately 0.1–5 $\mu\text{mol/g}$ tissue. In the current study, we used the 5 mM D-Asp solution at 10 ml/kg body weight for intragastric administration, which means 50 $\mu\text{mol/kg}$ body weight. This indicates that the concentration of D-Asp used in this study is within the range of the oral intake of natural products. The intragastric administration of 5 mM D-Asp increased D-Asp in

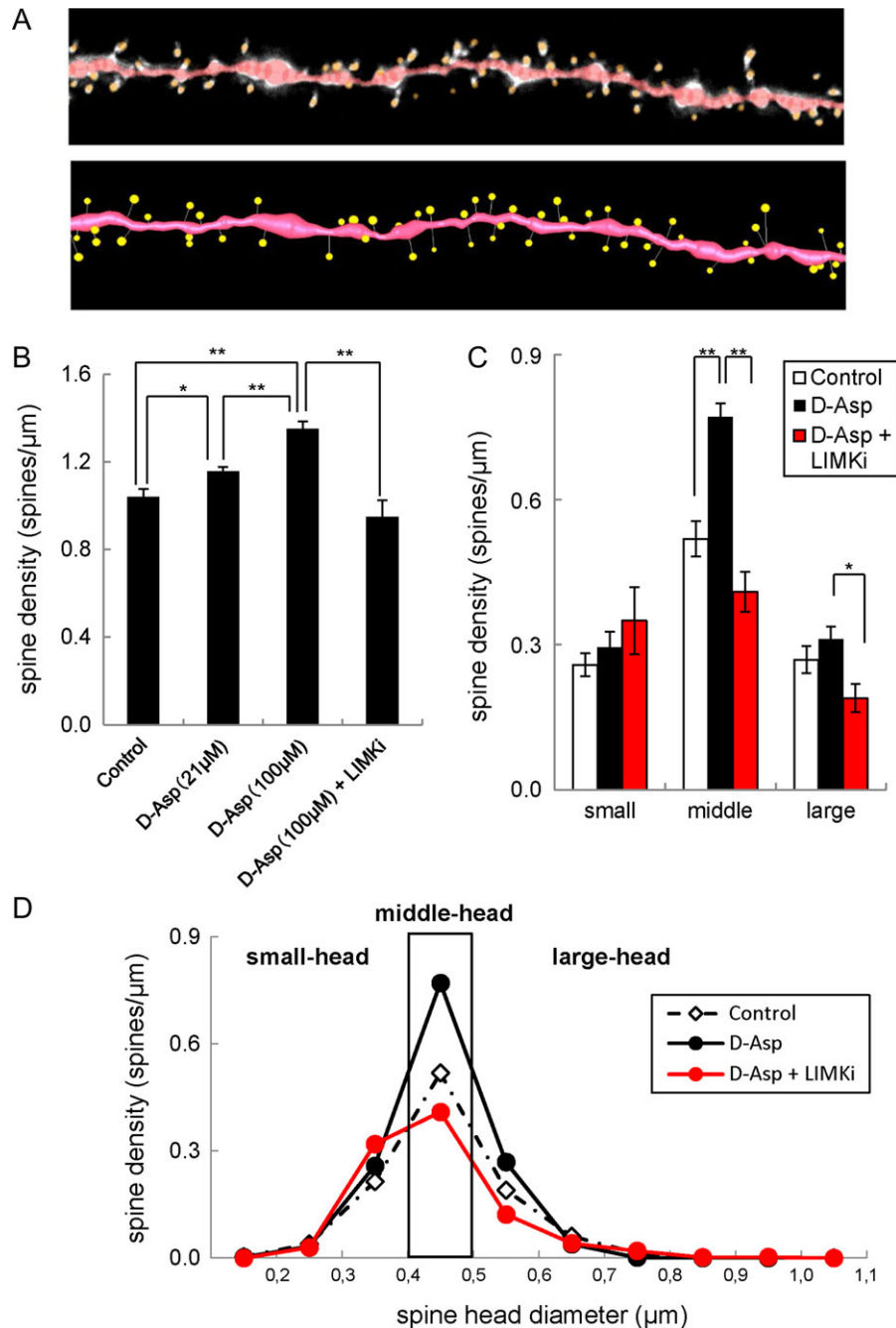


Figure 6. (A) 3D images of dendritic spines in CA1 hippocampal neurons after D-Asp treatments, analyzed by Spiso (upper), and 3D-reconstructed model (lower). (B) The total spine density after 2 h of treatment for control, 21 μM D-Asp, 100 μM D-Asp and 100 μM D-Asp + LIMKi (D-Asp + LIMKi). (C) The spine density of 3 subtypes after 2 h of treatment for control, 100 μM D-Asp (D-Asp) and 100 μM D-Asp + LIMKi (D-Asp + LIMKi). (D) Histograms of spine head diameters after 2 h treatment for control, 100 μM D-Asp (D-Asp) and 100 μM D-Asp + LIMKi (D-Asp + LIMKi). Horizontal axis, spine head diameter (D). Vertical axis, spine density (B–D). Results are represented as mean \pm SEM. Statistical significance yielded ** $P < 0.01$, * $P < 0.05$ with Tukey–Kramer multiple comparison test. For each drug treatments, we investigated 50 dendrites with 2300–2700 spines from 3 rats, 12 slices, 30 neurons.

the hippocampus to 21.29 nmol/g wet tissue (Fig. 5). In the previous study, we assumed that hippocampal tissue with a wet weight of 1 g has an approximate volume of 1 mL, as the majority of the tissue consists of water, with a weight per 1 mL of 1 g, and the volume should be decreased by less than 10% due to the proteins and lipids (0.7–0.8 mL/g) (Kimoto et al. 2001). The D-Asp concentration in the hippocampus following D-Asp administration is therefore estimated to be approximately 21 μM . This supports that the concentration of D-Asp

incubation in acute hippocampal slices (21–100 μM) is close to the physiological range.

Rapid Facilitation of Functional Connectivity and Spinogenesis in the Hippocampus by D-Asp

The hippocampal–cortical network, including the striatum, substantia nigra, and somatosensory cortex, is involved in the procedural memory process (Pennartz et al. 2011). In particular,

decreased synchronization between the hippocampus and the somatosensory cortex corresponds to the cognitive dysfunction and memory dysfunction that occur in an aged rat model (Xie et al. 2013; Ash et al. 2016). Additionally, the dendritic spines of CA1 neurons are involved in the memory process (Diamond et al. 2006). Therefore, increased synchronization in the hippocampal–cortical network and spinogenesis in the hippocampal CA1 neurons by D-Asp in the present study could support the improvement of memory function by D-Asp application in aged rats (Topo et al. 2010).

Rapid effects of D-Asp on the spinogenesis suggest that D-Asp may be a modulator of N-methyl-D-Asp (NMDA) receptors whose activity is also modulated by D-serine bound to glycine binding site (Mothet et al. 2000; Errico et al. 2014). Synaptic modulator hypothesis of D-Asp was also supported by D'Aniello et al. (2011).

Because the functional connectivity between hippocampus and the cortex can be facilitated with the NMDA agonist (Grimm et al. 2015), D-Asp possibly increased functional connectivity between the hippocampus and the cortex by interacting with NMDA receptors in the hippocampal neurons (Fig. 3). Interestingly, an intragastric administration of L-Asp does not activate the brain regions examined (Tsurugizawa et al. 2014). The intragastric administration of L-Asp increases the plasma level of L-Asp but not D-Asp (Finkelstein et al. 1983). Additionally, the transporter that conveys L-Asp from the blood vessels into the brain has been found (Smith 2000). Hence, distinct effect of L- and D-Asp on the neuronal activity in the hippocampus can be explained by different action on the NMDA receptors.

The LIMK-dependent signaling of spine increase via phosphorylation of cofilin is a crucial nongenomic pathway, leading to actin polymerization and spine formation (Meng et al. 2002, 2003; Hasegawa et al. 2015). Importantly, we have shown that NMDA-LIMK pathway is also involved in the acute, nongenomic spinogenesis by estrogen and androgen in rat hippocampal neurons (Hasegawa et al. 2015; Hatanaka et al. 2015). Here, we clearly showed that LIMK also bridged the acute spinogenesis triggered by D-Asp. Together, the mechanism of acute facilitation of the synaptic connectivity by D-Asp may be due to the nongenomic LIMK pathway and NMDA-mediated synaptic connectivity (Supplementary Fig. S1).

Conclusion

In conclusion, food-derived D-Asp, as opposed to L-Asp has a direct action on the hippocampal neurons to induce the macroscale functional connectivity and microscale synaptic plasticity. This study is the first report that focuses on the effects of D-Asp on functional connectivity and synaptic plasticity.

Supplementary Material

Supplementary material is available at *Cerebral Cortex* online.

Funding

Ajinomoto Co., Inc. and Kao Research Council.

Notes

We thank Mr. Tsuyoshi Tokita (A-TEC, Nishinomiya, Japan) for technical assistance with the MRI measurements. *Conflict of Interest*: None declared.

References

- Abe Y, Tsurugizawa T, Le Bihan D. 2017. Water diffusion closely reveals neural activity status in rat brain loci affected by anesthesia. *PLoS Biol.* 15:e2001494.
- Ash JA, Lu H, Taxier LR, Long JM, Yang Y, Stein EA, Rapp PR. 2016. Functional connectivity with the retrosplenial cortex predicts cognitive aging in rats. *Proc Natl Acad Sci USA.* 113: 12286–12291.
- Chang PC, Prociassi D, Bao Q, Centeno MV, Baria A, Apkarian AV. 2016. Novel method for functional brain imaging in awake minimally restrained rats. *J Neurophysiol.* 116:61–80.
- Diamond DM, Campbell AM, Park CR, Woodson JC, Conrad CD, Bachstetter AD, Mervis RF. 2006. Influence of predator stress on the consolidation versus retrieval of long-term spatial memory and hippocampal spinogenesis. *Hippocampus.* 16: 571–576.
- Dunlop DS, Neidle A, McHale D, Dunlop DM, Lajtha A. 1986. The presence of free D-aspartic acid in rodents and man. *Biochem Biophys Res Commun.* 141:27–32.
- D'Aniello A. 2007. D-Aspartic acid: an endogenous amino acid with an important neuroendocrine role. *Brain Res Rev.* 53: 215–234.
- D'Aniello S, Somorjai I, Garcia-Fernandez J, Topo E, D'Aniello A. 2011. D-Aspartic acid is a novel endogenous neurotransmitter. *FASEB J.* 25:1014–1027.
- Errico F, Nistico R, Di Giorgio A, Squillace M, Vitucci D, Galbusera A, Piccinin S, Mango D, Fazio L, Middei S, et al. 2014. Free D-aspartate regulates neuronal dendritic morphology, synaptic plasticity, gray matter volume and brain activity in mammals. *Transl Psychiatry.* 4:e417.
- Errico F, Nistico R, Napolitano F, Mazzola C, Astone D, Pisapia T, Giustizieri M, D'Aniello A, Mercuri NB, Usiello A. 2011. Increased D-aspartate brain content rescues hippocampal age-related synaptic plasticity deterioration of mice. *Neurobiol Aging.* 32:2229–2243.
- Finkelstein MW, Daabees TT, Stegink LD, Applebaum AE. 1983. Correlation of aspartate dose, plasma dicarboxylic amino acid concentration, and neuronal necrosis in infant mice. *Toxicology.* 29:109–119.
- Furuchi T, Homma H. 2005. Free D-aspartate in mammals. *Biol Pharm Bull.* 28:1566–1570.
- Grimm O, Gass N, Weber-Fahr W, Sartorius A, Schenker E, Spedding M, Risterucci C, Schweiger JI, Bohringer A, Zang Z, et al. 2015. Acute ketamine challenge increases resting state prefrontal-hippocampal connectivity in both humans and rats. *Psychopharmacology (Berl).* 232:4231–4241.
- Hasegawa Y, Hojo Y, Kojima H, Ikeda M, Hotta K, Sato R, Ooishi Y, Yoshiya M, Chung BC, Yamazaki T, et al. 2015. Estradiol rapidly modulates synaptic plasticity of hippocampal neurons: involvement of kinase networks. *Brain Res.* 1621: 147–161.
- Hashimoto A, Nishikawa T, Konno R, Niwa A, Yasumura Y, Oka T, Takahashi K. 1993. Free D-serine, D-aspartate and D-alanine in central nervous system and serum in mutant mice lacking D-amino acid oxidase. *Neurosci Lett.* 152:33–36.
- Hatanaka Y, Hojo Y, Mukai H, Murakami G, Komatsuzaki Y, Kim J, Ikeda M, Hiragushi A, Kimoto T, Kawato S. 2015. Rapid increase of spines by dihydrotestosterone and testosterone in hippocampal neurons: dependence on synaptic androgen receptor and kinase networks. *Brain Res.* 1621: 121–132.
- Hering H, Sheng M. 2001. Dendritic spines: structure, dynamics and regulation. *Nat Rev Neurosci.* 2:880–888.

- Hojo Y, Munetomo A, Mukai H, Ikeda M, Sato R, Hatanaka Y, Murakami G, Komatsuzaki Y, Kimoto T, Kawato S. 2015. Estradiol rapidly modulates spinogenesis in hippocampal dentate gyrus: involvement of kinase networks. *Horm Behav.* 74:149–156.
- Homma H. 2007. Biochemistry of D-aspartate in mammalian cells. *Amino Acids.* 32:3–11.
- Ikeda M, Hojo Y, Komatsuzaki Y, Okamoto M, Kato A, Takeda T, Kawato S. 2015. Hippocampal spine changes across the sleep-wake cycle: corticosterone and kinases. *J Endocrinol.* 226:M13–M27.
- Kanai Y, Hediger MA. 2003. The glutamate and neutral amino acid transporter family: physiological and pharmacological implications. *Eur J Pharmacol.* 479:237–247.
- Kimoto T, Tsurugizawa T, Ohta Y, Makino J, Tamura H, Hojo Y, Takata N, Kawato S. 2001. Neurosteroid synthesis by cytochrome p450-containing systems localized in the rat brain hippocampal neurons: N-methyl-D-aspartate and calcium-dependent synthesis. *Endocrinology.* 142:3578–3589.
- Lee MH, Smyser CD, Shimony JS. 2013. Resting-state fMRI: a review of methods and clinical applications. *AJNR Am J Neuroradiol.* 34:1866–1872.
- Maletic-Savatic M, Malinow R, Svoboda K. 1999. Rapid dendritic morphogenesis in CA1 hippocampal dendrites induced by synaptic activity. *Science.* 283:1923–1927.
- Meng Y, Zhang Y, Tregoubov V, Falls DL, Jia Z. 2003. Regulation of spine morphology and synaptic function by LIMK and the actin cytoskeleton. *Rev Neurosci.* 14:233–240.
- Meng Y, Zhang Y, Tregoubov V, Janus C, Cruz L, Jackson M, Lu WY, MacDonald JF, Wang JY, Falls DL, et al. 2002. Abnormal spine morphology and enhanced LTP in LIMK-1 knockout mice. *Neuron.* 35:121–133.
- Ming GL, Song H. 2005. Adult neurogenesis in the mammalian central nervous system. *Annu Rev Neurosci.* 28:223–250.
- Morikawa A, Hamase K, Inoue T, Konno R, Zaitus K. 2007. Alterations in D-amino acid levels in the brains of mice and rats after the administration of D-amino acids. *Amino Acids.* 32:13–20.
- Mothet JP, Parent AT, Wolosker H, Brady RO Jr., Linden DJ, Ferris CD, Rogawski MA, Snyder SH. 2000. D-serine is an endogenous ligand for the glycine site of the N-methyl-D-aspartate receptor. *Proc Natl Acad Sci USA.* 97:4926–4931.
- Mukai H, Hatanaka Y, Mitsushashi K, Hojo Y, Komatsuzaki Y, Sato R, Murakami G, Kimoto T, Kawato S. 2011. Automated analysis of spines from confocal laser microscopy images: application to the discrimination of androgen and estrogen effects on spinogenesis. *Cereb Cortex.* 21:2704–2711.
- Mukai H, Tsurugizawa T, Murakami G, Kominami S, Ishii H, Ogiue-Ikeda M, Takata N, Tanabe N, Furukawa A, Hojo Y, et al. 2007. Rapid modulation of long-term depression and spinogenesis via synaptic estrogen receptors in hippocampal principal neurons. *J Neurochem.* 100:950–967.
- Pan WJ, Billings JC, Grooms JK, Shakil S, Keilholz SD. 2015. Considerations for resting state functional MRI and functional connectivity studies in rodents. *Front Neurosci.* 9:269.
- Paxinos G, Watson C. 1998. The rat brain in stereotaxic coordinates. 4th ed. San Diego (CA): Academic Press.
- Pennartz CM, Ito R, Verschure PF, Battaglia FP, Robbins TW. 2011. The hippocampal-striatal axis in learning, prediction and goal-directed behavior. *Trends Neurosci.* 34:548–559.
- Sato M, Inoue F, Kanno N, Sato Y. 1987. The occurrence of N-methyl-D-aspartic acid in muscle extracts of the blood shell, *Scapharca broughtonii*. *Biochem J.* 241:309–311.
- Schell MJ, Cooper OB, Snyder SH. 1997. D-aspartate localizations imply neuronal and neuroendocrine roles. *Proc Natl Acad Sci USA.* 94:2013–2018.
- Segal M. 2005. Dendritic spines and long-term plasticity. *Nat Rev Neurosci.* 6:277–284.
- Shibata K, Tarui A, Todoroki N, Kawamoto S, Takahashi S, Kera Y, Yamada R. 2001. Occurrence of N-methyl-L-aspartate in bivalves and its distribution compared with that of N-methyl-D-aspartate and D,L-aspartate. *Comp Biochem Physiol B Biochem Mol Biol.* 130:493–500.
- Shinohara Y, Hirase H, Watanabe M, Itakura M, Takahashi M, Shigemoto R. 2008. Left-right asymmetry of the hippocampal synapses with differential subunit allocation of glutamate receptors. *Proc Natl Acad Sci USA.* 105:19498–19503.
- Smith QR. 2000. Transport of glutamate and other amino acids at the blood-brain barrier. *J Nutr.* 130:1016S–1022S.
- Topo E, Soricelli A, Di Maio A, D’Aniello E, Di Fiore MM, D’Aniello A. 2010. Evidence for the involvement of D-aspartic acid in learning and memory of rat. *Amino Acids.* 38:1561–1569.
- Tsurugizawa T, Uematsu A, Uneyama H, Torii K. 2009. Blood oxygenation level-dependent response to intragastric load of corn oil emulsion in conscious rats. *Neuroreport.* 20:1625–1629.
- Tsurugizawa T, Uematsu A, Uneyama H, Torii K. 2010a. Effects of isoflurane and alpha-chloralose anesthesia on BOLD fMRI responses to ingested L-glutamate in rats. *Neuroscience.* 165:244–251.
- Tsurugizawa T, Uematsu A, Uneyama H, Torii K. 2010b. The role of the GABAergic and dopaminergic systems in the brain response to an intragastric load of alcohol in conscious rats. *Neuroscience.* 171:451–460.
- Tsurugizawa T, Uematsu A, Uneyama H, Torii K. 2012. Functional brain mapping of conscious rats during reward anticipation. *J Neurosci Methods.* 206:132–137.
- Tsurugizawa T, Uematsu A, Uneyama H, Torii K. 2013. Reversible brain response to an intragastric load of L-lysine under L-lysine depletion in conscious rats. *Br J Nutr.* 109:1323–1329.
- Tsurugizawa T, Uneyama H. 2014. Differences in BOLD responses to intragastrically infused glucose and saccharin in rats. *Chem Senses.* 39:683–691.
- Tsurugizawa T, Uneyama H, Torii K. 2014. Brain amino acid sensing. *Diabetes Obes Metab.* 16(Suppl 1):41–48.
- Uematsu A, Kitamura A, Iwatsuki K, Uneyama H, Tsurugizawa T. 2015. Correlation between activation of the prelimbic cortex, basolateral amygdala, and agranular insular cortex during taste memory formation. *Cereb Cortex.* 25:2719–2728.
- Visser WF, Verhoeven-Duif NM, Ophoff R, Bakker S, Klomp LW, Berger R, de Koning TJ. 2011. A sensitive and simple ultra-high-performance-liquid chromatography-tandem mass spectrometry based method for the quantification of D-amino acids in body fluids. *J Chromatogr A.* 1218:7130–7136.
- Xie P, Yu T, Fu X, Tu Y, Zou Y, Lui S, Zhao X, Huang X, Kemp GJ, Gong Q. 2013. Altered functional connectivity in an aged rat model of postoperative cognitive dysfunction: a study using resting-state functional MRI. *PLoS One.* 8:e64820.
- Yoshida K, Mimura Y, Ishihara R, Nishida H, Komaki Y, Minakuchi T, Tsurugizawa T, Mimura M, Okano H, Tanaka KF, et al. 2016. Physiological effects of a habituation procedure for functional MRI in awake mice using a cryogenic radiofrequency probe. *J Neurosci Methods.* 274:38–48.